AIAA-91-0216
EXPERIENCE WITH TWO-LAYER MODELS COMBINING THE k-ε MODEL WITH A ONE-EQUATION MODEL NEAR THE WALL

W. Rodi
University of Karlsruhe
Karlsruhe, Germany

29th Aerospace Sciences Meeting

January 7–10, 1991/Reno, Nevada

AIAA-91-0216

Experience with Two-Layer Models Combining the k-ε Model with a One-Equation Model Near the Wall

W. Rodi*

Institute for Hydromechanics
University of Karlsruhe
D-7500 Karlsruhe, F.R. Germany

Abstract

The paper reports on experience gathered so far with the use of two-layer turbulence models combining the k-ε model with a one-equation model near the wall. The various models of this type proposed in the literature all use the same standard k-ε model in the bulk of the flow away from the wall, but somewhat different one-equation models for simulating the viscosity-affected near-wall region. The various formulations are presented and discussed briefly. The performance of two-layer models is demonstrated with the aid of application examples for a variety of two-dimensional boundary-layer and separated flows. Whenever possible, the results are compared with calculations obtained with the k-ε model using wall functions or a low-Re k-ε model near the wall, and the relative merits of the two-layer model vis-à-vis these model versions are discussed.

1. Introduction

The k-ε model is presently the most widely used turbulence model for practical calculations and has been built into virtually all commercial general-purpose CFD codes. Most calculations carried out so far with the k-ε model were done by bridging the viscosity-affected near-wall layers by wall functions. This approach, which is also adopted in most commercial codes, was used for two reasons: The numerical resolution of the thin near-wall layers with steep gradients was beyond the available computer resources, at least for more complex flows with separation, and the standard k-ε model involving fixed constants is not applicable in the viscosity-affected region. Instead of resolving this region, the first grid point away from the wall is therefore placed outside the viscous sublayer. As desribed in detail in Ref. 1, wall functions relate the velocity as well as the turbulence parameters k and ε at the first grid point mainly to the friction velocity and lean heavily on the assumption of a logarithmic velocity distribution and the validity of local equilibrium of turbulence (production = dissipation) at this point. These assumptions are certainly not generally valid, for example not when strong secondary flows extend into the sublayer[2], and also not in separated flows. Fig. 1 shows measured velocity distributions in wall coordinates in the reverse-flow region behind a step and a fence in comparison with the standard logarithmic distribution. It is clear that the measured profile deviates significantly from the logarithmic distribution. Fig. 2 exhibits the measured turbulent kinetic energy balance in the same region behind a step (albeit for a different experimental situation) and this figure demonstrates clearly that near the wall there is no balance between production and dissipation but rather between dissipation and diffusion so that the assumption of local equilibrium is invalid. Wall functions involving the friction velocity are of course

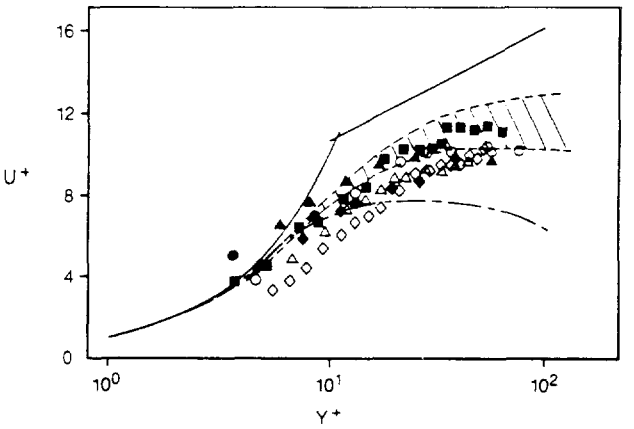

Fig. 1: Near-wall velocity distribution in reverse flow regions; symbols: measurements in backward facing step flow[3],shaded area: measurements in flow over fence[4], — log-linear distribution, — . — 2-layer-model calculations in step flow[22]

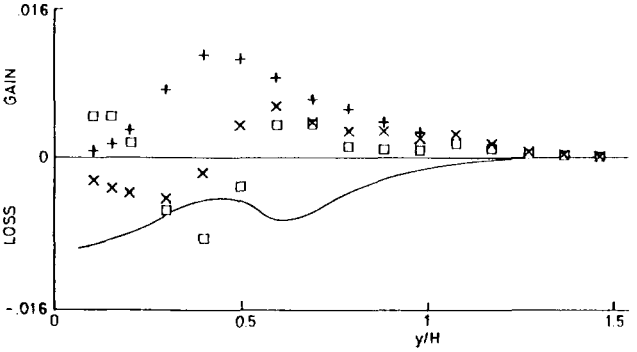

Fig. 2: Measured turbulent kinetic energy balance in backward facing step flow 2.1 step heights upstream of reattachment[5]; + Production, x Convection, □ Diffusion, — Dissipation by difference

particularly unsuited for separation and reattachment regions where the friction velocity changes sign.

Due to recent increases in computer power, the necessity to use wall functions was much reduced, and considerable activity has recently been directed towards the development and testing of low-Reynolds-number models for simulating the turbulent processes very near walls. For making the k-ε model applicable to the viscosity-affected near-wall region, the standard high-Reynolds-number version had to be modified by replacing some of the constants by viscosity-dependent functions (although the near-wall damping of the eddy viscosity simulated by one of these is really due to an inviscid mechanism[6]) and additional terms in the k- and ε-equations. A variety of low-Reynolds-number k-ε models involving different functions and additional terms have been proposed, and the pre-1984 models have been reviewed by Patel et al.[7]. More recent proposals are compiled in Ref. 8. All versions have been tested mainly in boundary-layer flows, and some are now routinely used in industrial calculations[9]. Depending somewhat on the version considered, low-Reynolds-number k-ε models were found to require rather high numerical resolution near the wall, mainly because of the steep gradient of the dissipation rate ε, whose distribution is determined by solving a transport equation for this quantity. Typically 60 to 100 grid points across boundary layers are required for proper numerical resolution. In spite of the recent advances in computer power, this means that in general 3D flows involving several walls, the limits of available computer resources are reached quickly. Further, k-ε models have been found to perform rather poorly in boundary layers with adverse pressure gradient[10] (see Fig. 7 below). On the other hand, one-equation models with a standard empirical prescription of the length scale near the wall work quite well for these flows[10]. In separated flows, the low-Re versions of the k-ε model are little tested so far. Initial calculations indicated that the damping functions developed for attached boundary layers are not always well behaved in these flows.

In order to save grid points and hence computer storage and time, to increase the robustness of the method, and also to introduce the fairly well established length-scale distribution very near walls into the model, a recent trend has been to use the k-ε model only away from the wall and resolve the viscosity-affected near-wall layer with a simpler model involving a length-scale prescription. This is the two-layer approach considered in the present paper. Iacovides and Launder[2] employed the van Driest version of the mixing-length model in combination with both the standard k-ε and an algebraic stress model to calculate the flow and heat transfer in a pipe rotating in orthogonal mode. Chen and Patel[11,12] combined the one-equation model of Wolfshtein[13] for the viscous sublayer with the k-ε model and calculated the evolution of the flows past a prolate spheroid and an afterbody with small separation regions. The same model combination was also adopted by Launder and his co-workers[14,15] to calculate various flows. Instead of the Wolfshtein model, the author and his colleagues combined the Norris-Reynolds[16] one-equation model with the k-ε model to form a two-layer model because the Norris-Reynolds model was found to perform well in boundary layers with adverse pressure gradient[10] and transpiration[17]. The present paper reports on the experience gathered so far with the two-layer approach and discusses the achievements and limitations with the aid of a number of calculation examples.

2. Form of Two-Layer Models

The two-layer models discussed here employ the standard high-Reynolds-number k-ε model in the bulk of the flow not too close to walls. This model is based on the eddy-viscosity concept and calculates the distribution of the eddy viscosity from

$$\nu_t = c_\mu \frac{k^2}{\varepsilon} \tag{1}$$

The distributions of the turbulence parameters k (turbulent kinetic energy) and ε (dissipation rate) are calculated from the following model equations governing these quantities:

$$\frac{\partial k}{\partial t} + U_j \frac{\partial k}{\partial x_j} = \frac{\partial}{\partial x_j}\left[(\nu + \frac{\nu_t}{\sigma_k})\frac{\partial k}{\partial x_j}\right] + \underbrace{\nu_t \left(\frac{\partial U_i}{\partial x_j} + \frac{\partial U_j}{\partial x_i}\right)\frac{\partial U_i}{\partial x_j}}_{P_k} - \varepsilon \tag{2}$$

$$\frac{\partial \varepsilon}{\partial t} + U_j \frac{\partial \varepsilon}{\partial x_j} = \frac{\partial}{\partial x_j}\left(\frac{\nu_t}{\sigma_\varepsilon}\frac{\partial \varepsilon}{\partial x_j}\right) + c_{\varepsilon 1}\frac{\varepsilon}{k}P_k - c_{\varepsilon 2}\frac{\varepsilon^2}{k} \tag{3}$$

In the k-equation, the molecular viscosity ν appearing in the diffusion term is negligible compared with ν_t/σ_k in high-Reynolds-number regions where the standard k-ε model is applied. The standard values are employed for the constants appearing in this model (c_μ = 0.09, $c_{\varepsilon 1}$ = 1.44, $c_{\varepsilon 2}$ = 1.92, σ_k = 1.0, σ_ε = 1.3).

The viscosity-affected regions near walls are resolved with a one-equation turbulence model. In this, the dissipation rate ε appearing as length-scale-determining variable in the eddy viscosity relation (1) and as source term in the kinetic energy equation (2) is not determined from a transport equation but from a prescribed length-scale distribution. Specifically, the eddy-viscosity relation (1) is rewritten as:

$$\nu_t = c_\mu k^{1/2} \ell_\mu \tag{4}$$

and ε is determined from

$$\varepsilon = \frac{k^{3/2}}{\ell_\varepsilon} \tag{5}$$

When the coefficient c_μ in (4) is chosen as the square of the structure parameter $\overline{u\,v}/k$ under local equilibrium conditions in shear layers, the length scales ℓ_μ and ℓ_ε are the same in the log-law region, where they vary linearly. Very close to the wall, deviations from the linear distribution occur, and these are different for ℓ_μ and ℓ_ε. The observed damping of the eddy viscosity very near walls is effected by a reduction of ℓ_μ with the aid of an exponential function similar to the van Driest damping function used in the mixing-length model. Both the Wolfshtein and the Norris-Reynolds model employ the following relation for ℓ_μ:

$$\ell_\mu = C_\ell\, y \left(1 - \exp(-\frac{Re_y}{A_\mu}\frac{25}{A^+})\right) \tag{6}$$

This involves the argument

$$Re_y = \frac{k^{1/2} y}{\nu} \tag{7}$$

which in constrast to the original van Driest function does not involve the friction velocity U_τ and hence is applicable also to separated flows. For conformity with the log law, the constant C_ℓ is chosen as:

$$C_\ell = \kappa c_\mu^{-3/4} \tag{8}$$

where c_μ is the same constant as in the k-ε model (= 0.09) and κ is the von Kármán constant which is chosen somewhat differently by different modellers. The constant A_μ in the damping function was also chosen differently by various modellers: Patel and co-workers[11,12] adopted A_μ = 70, Launder and co-workers[14,15] chose A_μ = 62.5 and in the Norris-Reynolds model employed in the author's group a value of A_μ = 50.5 is employed. In most cases, the additional parameter A^+ is given a value of 25; only in the work of Fujisawa et al.[18] is this parameter allowed to deviate from a value of 25 in order to account for the effects of favourable pressure gradients and laminar-turbulent transition. This will be discussed in

It should be noted here that the damping of the eddy viscosity effected by the viscosity-dependent exponential function in (6) is not really a viscous effect but is a result of the near-wall reduction of the normal fluctuations $\overline{v^2}$ due to a pressure-strain mechanism, as was discussed by Launder[6] and Durbin[19]. This was recently confirmed also by an evaluation of direct simulation data for turbulent bounday-layer and channel flow[20]. Nevertheless, in all existing one-equation models, the damping of eddy viscosity is simulated with the aid of the viscosity-dependent function (6).

The relations for prescribing the length scale ℓ_ε in the dissipation relation (5) also involve a damping below the linear distribution. Here, different damping functions were proposed. In Wolfshtein's[13] model, an exponential function similar to the one used in (6) is employed:

$$\ell_\varepsilon = C_\ell\, y \left(1 - \exp(-\frac{Re_y}{A_\varepsilon})\right) \tag{9}$$

For the damping constant A_ε, Launder and co-workers[14,15] use a value of A_ε = 3.8 and Patel and co-workers[11,12] a value of $A_\varepsilon = 2C_\ell$ = 5.08. Norris and Reynolds[16] proposed a different damping function, and their ℓ_ε prescription reads:

$$\ell_\varepsilon = \frac{C_\ell\, y}{1 + 5.3/Re_y} \tag{10}$$

It can be verified that this ℓ_ε-function goes much slower to the linear distribution than the damping function (9) due to Wolfshtein. A recent evaluation of direct numerical simulation (DNS) data[20] has shown that the damping of ℓ_ε according to relations (9) and (10) is not in agreement with DNS data for channel and boundary-layer flow. These data rather suggest that ℓ_ε increases near the wall beyond the linear distribution $\ell_\varepsilon = C_\ell\, y$. This can be understood from the ε-distributions given in Fig. 3. According to the DNS data, ε has its maximum value at the wall, and its distribution has a plateau at $y^+ \approx 12$ while the one-equation models with a ℓ_ε-distribution according to (9) or (10) (but also existing low-Re k-ε models) produce an ε-peak in this region and a lower value at the wall. The latter behaviour was previously also inferred from experimental data (see Patel et al[7]), but the reliability of these is probably not very high very near the wall. The disagreement in the ε-distribution between existing one-equation models and the DNS data should be kept in mind, but it has probably little adverse effect on the prediction of flow quantities of engineering interest.

In general flow situations, the appearance of the wall distance y in the argument Re_y of the damping functions is not ideal, and hence Yap[14] has experimented with the alternative argument $\tilde{Re}_t = k^2/\tilde{\varepsilon}\nu$, where $\tilde{\varepsilon}$ is a modified dissipation rate defined by $\tilde{\varepsilon} = \varepsilon - \nu\,(\partial k^{1/2}/\partial y)^2$. The superiority of this approach could not be established and hence it has not become very popular. It should be added here that, if one-equation models are used for the entire shear layer (rather than only in the near-wall region) a ramp function is adopted for the length scales with $\ell_\mu = \ell_\varepsilon$ = const. x δ in the outer region, where δ is the shear-layer thickness.

In two-layer modelling, the two models have to be

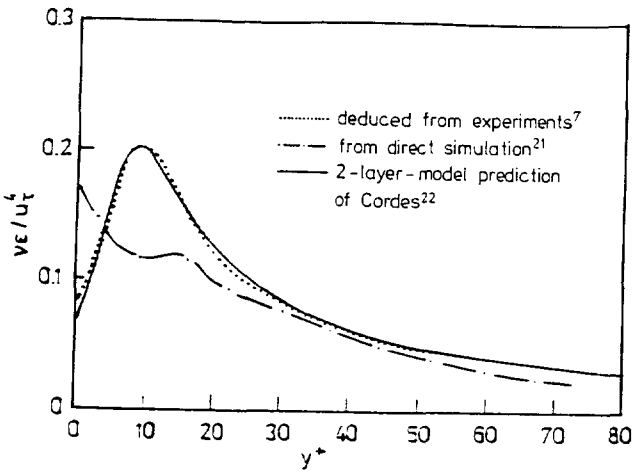

Fig. 3: Distribution of dissipation rate ε near wall in channel flow

matched at some location, and this should be placed near the edge of the viscous sublayer, i.e. in a region where viscous effects have become negligible. Launder and Patel and their co-workers match the two models at preselected grid lines running along the wall. Yap[14] is not very specific and mentions only that six or more nodes were placed across the one-equation-model region. Iacovides and Launder[15] used ten nodes in this region and report that the matching took place in a y^+-region of 80 to 120. Patel and co-workers[11,12] match along a grid line where the minimum of Re_y is of the order of 250. They found that the results are not sensitive to the matching criterion as long as the minimum value of Re_y was greater than 200. It should be noted that in normal boundary-layer flow Re_y = 250 corresponds roughly to y^+ = 135. The author and his co-workers do not match the two models at a preselected grid line but at a location where a certain criterion is satisfied. Two criteria have been tested: one is to match the models at a location where the ratio of eddy viscosity to molecular viscosity has a certain (relatively high) value. ν_t/ν ratios in the range of 12 to 48 have been tested[22], and the calculation results were found independent of the exact matching criterion when the ratio was beyond 30. The second criterion was to match the models where the damping function in the length-scale relation (6), i.e. the expression in paranthesis has a value close to unitiy so that the viscous effects are small. For the calculations a value of 0.95 was chosen. In boundary layers these matching criteria effectively led to a switching between the models at y^+ = 80 - 90. The matching with either of the last mentioned criteria should be more generally applicable than the matching at a preselected grid line.

3. Application Examples

3.1 Two-Dimensional Boundary Layers

Fujisawa et al.[18] calculated a variety of two-dimensional boundary layers with the 2-layer model in use in the author's group and compared their results with experiments as well as with their calculations obtained with the Lam-Bremhorst low-Re k-ε model and the Norris-Reynolds one-equation model applied over the full boundary-layer width. In their two-layer-model calculations , the two models were matched at a wall distance where the damping function in (6), which is the expression in parenthesis, adopts a value of 0.95.

Boundary-Layers with Zero Pressure Gradient. All three turbulence models tested by Fujisawa et al[18] predict quite well the development of the friction coefficient in the zero-pressure-gradient boundary-layer experiment of Wieghardt and Tillmann, whose data are given in Coles and Hirst[23]. Fig. 4 shows how well the models predict the velocity distribution in wall coordinates. The two-layer model calculations follow quite well the log-law in the intermediate y^+-region, but the logarithmic distribution is approached somewhat too slowly and in the outer region the deviation from the log-law is not strong enough. In Fig. 5 the predicted kinetic energy profiles are compared with the measurements of Klebanoff[24]. All three models can be seen to reproduce the data very well except very close to the wall. There the one-equation model gives too low a peak and would have to be adjusted for a better reproduction of the measured behaviour. The low-Re k-ε model predicts the peak nearly correctly as it was tuned to this effect. On the other hand, the Norris-Reynolds one-equation model and hence also the two-layer model simulate the near-wall shear-stress distribution very well, as is shown in Fig. 6. The shear stress predicted with the low-Re k-ε model approaches zero too quickly very near the wall. In this context it should be mentioned that, in their contribution to the Collaborative-Testing-of-Turbulence-Model effort, Patel and co-workers[25] obtained with their 2-layer model very good agreement for the velocity and shear-stress profiles with the direct numerical simulation data of Spalart[26] for boundary layers up to a momentum Reynolds-number thickness of 1410.

As the near-wall behaviour in developed channel and pipe flow is virtually the same as in boundary layers with zero pressure gradient, calculations of these flows deserve mention here. Cordes[22] calculated high-Re developed channel flow with basically the same two-

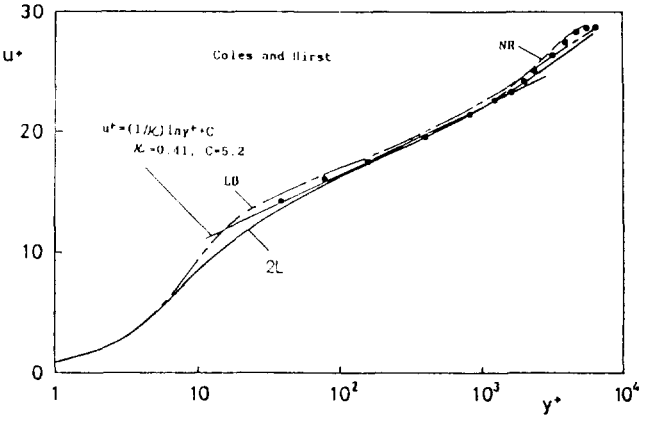

Fig. 4: Mean-velocity distribution in boundary layer with dP/dx = 0; lines are calculations[18] (LB = Lam-Bremhorst low-Re k-ε model, 2L = 2-layer model), data from Coles and Hirst[23]

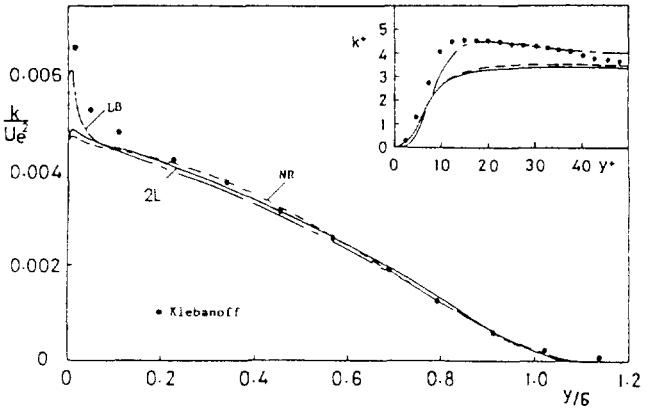

Fig. 5: Turbulent kinetic energy distribution in boundary layer with dP/dx = 0; calculations from Ref. 18, ● data[24]

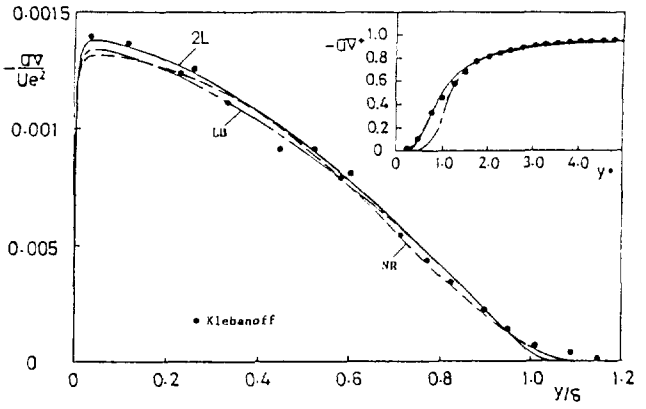

Fig. 6: Turbulent shear stress distribution in boundary layer with $dP/dx = 0$; calculations from Ref. 18, ● data[24]

layer model as was used by Fujisawa et al[18] and obtained virtually the same profiles as shown in Figs. 4 - 6. Yap[14] from Launder's group calculated developed pipe flow for the Reynolds numbers 5000, 42000 and 100000 with the two-layer model in use in this group. For the two larger Reynolds numbers, the standard logarithmic distribution was quite well recovered, but for Re = 5000 the calculated velocity profile fell below the logarithmic distribution. This trend is opposite to experimental observations. Perhaps the switching to the high-Re k-ε model some distance from the wall is not justified for this low Reynolds number flow, but since no details on the matching location are given this explanation must remain speculative.

Boundary Layers with Pressure Gradients. The situation studied experimentally by Samuel and Joubert[27] is the most often used test case for adverse-pressure-gradient boundary layers. For this case, Fig. 7 compares the calculations of Fujisawa et al.[18] obtained with three turbulence models with the data. The figure demonstrates once more a well known weakness of k-ε

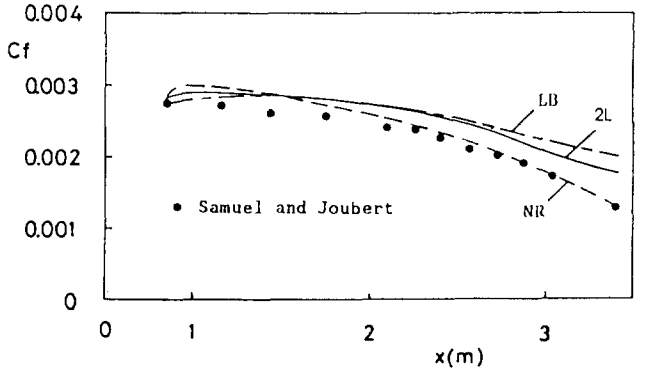

Fig. 7: Friction coefficient in boundary layer with adverse pressure gradient, lines are calculations[18], ● data[27]

models, namely to overpredict the friction coefficient c_f under adverse-pressure-gradient conditions. This behaviour was traced by Rodi and Scheuerer[10] to the high-Re form of the ε-equation (and in particular to the value of the coefficient $c_{\varepsilon 1}$ in this equation) which leads to a too steep increase of the turbulent length scale under these conditions. Fig. 7 shows that the prediction with the Norris-Reynolds one-equation model using a linear length-scale prescription near the wall predicts the friction coefficient correctly. The mixture of the two models used in the two-layer approach brings only some improvement over the k-ε-model prediction; over a large portion of the boundary layer the length scale is still determined by the ε-equation and hence predicted too high. Patel and co-workers[25] computed the same test case for the Collaborative-Testing-of-Turbulence-Model effort and report a c_f-distribution which actually falls slightly below the data. There is some indication that they match the two models considerably further away from the wall so that a larger portion of the boundary layer is covered by the one-equation model which can then exercise its beneficial influence. For the equilibrium boundary layer in adverse-pressure gradients studied experimentally by Bradshaw[28], Patel and Richman[29] also simulated the experimental data fairly well with the same two-layer model.

For strongly accelerating boundary layers leading to relaminarisation, low-Re k-ε models are known to perform quite well[17] and this can be seen also from Fig. 8 where Fujisawa et al's[18] calculations with three models are compared with data for the case studied experimentally by Badri Narayaran and Ramjee[30]. On the other hand, one-equation models in their original form cannot simulate well relaminarisation[31]. This can be remedied by introducing the effect of the pressure gradient on the damping function in the length-scale formula (6) through the coefficient A^+ which is a dimensionless sublayer thickness. As was suggested by Crawford and Kays[32] for the van Driest damping function, Fujisawa et al introduced the following dependence of A^+ on the pressure gradient:

$$A^+ = 25(30.175\, p^+ + 1) \quad , \; p^+ = \frac{\nu}{\rho U_\tau^3}\frac{dP}{dx} \tag{11}$$

The two-layer-model calculations shown in Fig. 8 were obtained with this function in the lenth-scale relation (6) and can be seen to give very similar results to those obtained with the k-ε model. Hence, with this function good agreement is achieved also for strongly accelerating boundary layers.

Transitional Boundary Layers. For the prediction of laminar-turbulent transition occurring for example on airfoils and turbine blades, the wall-function approach is not applicable and the use of a low-Reynolds-number model is an absolute necessity. Low-Reynolds-number k-ε models had some success in simulating transition at higher free-stream turbulence levels where transition occurs in a bypass situation due to the turbulent free-stream disturbances. Transition at low free-stream turbulence levels (say below 1%) occurring via shear-layer instability cannot be simulated by any statistical turbulence model and requires artificial triggering. For general transition calculations with the two-layer model, the author and

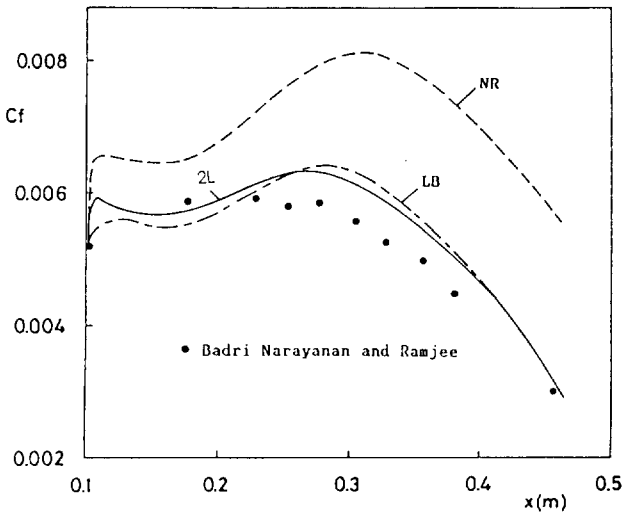

Fig. 8: Friction coefficient in strongly accelerating boundary layer, lines are calculations[18], ● data

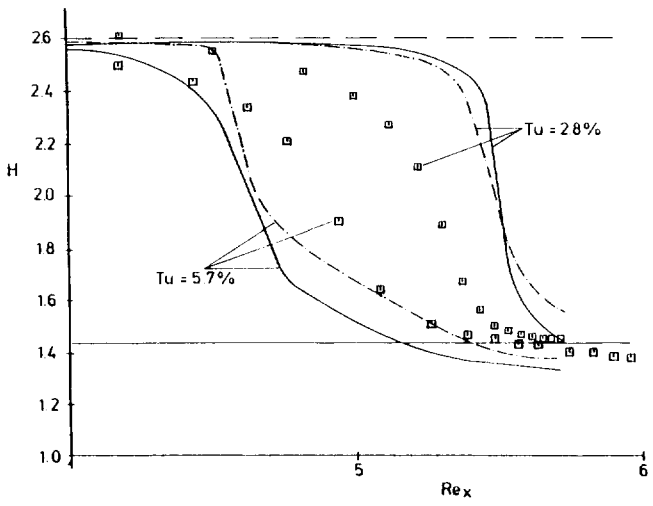

Fig. 9: Shape factor H in transitional boundary layers with dP/dx = 0; calculations[34]: — LB low-Re k-ε model, — . — two-layer model, □ data[35]

his co-workers adopted the following approach: The parameter A^+ occurring in the damping function in the length-scale relation (6) is made a function of the boundary-layer state. In laminar boundary layers, a large value is chosen for A^+ (here 300) so that a small eddy viscosity results, and for fully turbulent boundary layers A^+ is made a function of the pressure gradient according to relation (11), but with a value of 25 for zero and adverse pressure gradients. In the region of laminar-turbulent transition, A^+ is assumed to vary between these two limiting values according to the formula

$$A^+ = A_t^+(300 - A_t^+)\left(1 - \sin(\frac{\pi}{2}\frac{Re_\theta - Re_{tr}}{Re_{tr}})\right)^3 \qquad (12)$$

which is applied whenever the local momentum thickness Reynolds number Re_θ is larger than the critical transition Reynolds number Re_{tr} but smaller than twice this number. For the critical Reynolds number, the following empirical dependence on the free-stream turbulence level and the pressure gradient due to Abu Ghannam and Shaw[32] is taken:

$$Re_{tr} = 163 + \exp\left(F(\lambda_2) - \frac{F(\lambda_2)\cdot Tu}{6.91}\right) \qquad (13)$$

$$F(\lambda_2) = \begin{cases} 6.91 + 12.75\,\lambda_2 + 63.64\,\lambda_2^2, \lambda_2 \le 0 \\ 6.91 + \ 2.48\,\lambda_2 - 12.27\,\lambda_2^2, \lambda_2 > 0 \end{cases} \qquad \lambda_2 = -\frac{\Theta^2}{\mu_t \cdot U_e}\frac{dP}{dx}$$

where θ is the momentum thickness.

In a blind test for a workshop held at Lausanne[34], this model was applied to two transitional boundary layers on flat plates with different free-stream turbulence level. Predicted and measured distributions of the shape factor H are shown in Fig. 9, and predictions obtained with the Lam-Bremhorst low-Re k-ε model are also included. It can be seen that in this real prediction the drop in the shape factor H indicating transition is predicted reasonably well, but somewhat too late in the case of the lower free-stream-turbulence level. For a transitional boundary layer with adverse-pressure gradient and a free-stream turbulence level of 1.8%, the results of Fujisawa et al[18] show a similar performance. These authors were interested mainly in the influence of transition on heat transfer, and a few of their heat transfer calculations will now be presented. Fig. 10 compares the variation of the Stanton number predicted with the Lam-Bremhorst (LB) k-ε model and the two-layer (2L) model for boundary layers with zero pressure gradient at various free-stream turbulence levels with the data of Blair and Werle[36]. At the lowest turbulence level (1.3%), the LB-model predicts transition somewhat too late while the

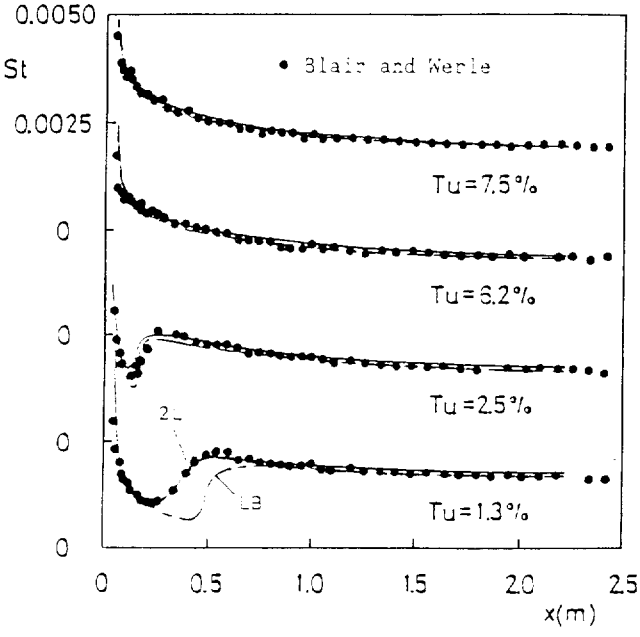

Fig. 10: Stanton number St in transitional boundary layers at dP/dx = 0, lines are calculations[18], ● data[36]

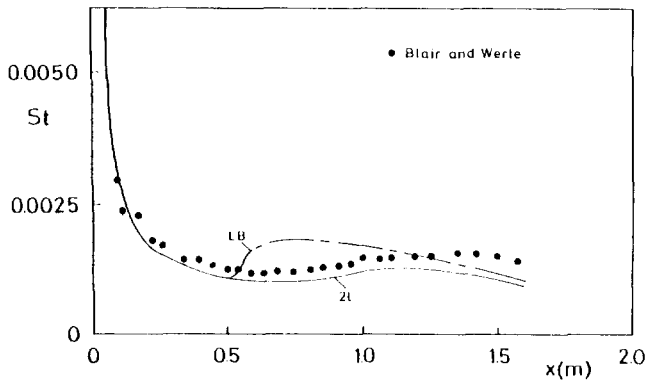

Fig. 11: Stanton number in transitional boundary layer with acceleration ($k = \nu U_e \cdot dU_e/dx = 0.75 \times 10^{-6}$), Tu = 2.1%; lines are calculations[18], ● data[37]

two-layer model yields very good agreement with the data. When the turbulence level is raised to 2.5%, transition moves forward and is predicted fairly well by both models. For the higher turbulence levels (6.2% and 7.5%), transition occurred before the first measurement station in the unheated wall part very close to the leading edge. This very early transition is predicted by both models. Fig. 11 provides the distribution of the Stanton number for a strongly accelerated boundary layer. Here this acceleration at modest free-stream turbulence level (2.1%) causes a delay in the onset of transition and also transition to take place over a larger distance than in the zero-pressure gradient case of Fig. 10. In this case, the LB low-Re k-ε model predicts transition to occur too early and too abruptly and only the two-layer model appears to do justice to the observed transition process.

The two-layer model has also been applied to simulate unsteady transition on a flat plate due to wakes moving over the plate. This is an idealisation of the boundary-layer flow on turbine blades exposed to the wakes generated by the preceding stage of the turbine. Rodi et al[38] used the transition model described above in a Lagrangean way, following fluid elements on their travel downstream, thereby comparing the local momentum thickness Reynolds number with the critical Reynolds number according to equation (13). The model allows to simulate the intermittent state of the boundary layer in this situation, and an application to unsteady boundary layers on turbine blades is in progress.

3.2 Two-Dimensional Separated Flows

The backward-facing step flow sketched in Fig. 12a, for which detailed experimental investigations were carried out by Driver and Seegmiller[5] for two angles of the upper wall ($\alpha = 0^o, 6^o$) was a test case at the 1980/81 Stanford Conference on Turbulent Flows and serves again as test case for the current Collaborative Testing of Turbulence Models effort. The flow was calculated with the two-layer model used in the author's group as well as with the standard k-ε model by Cordes[22] (only for $\alpha = 0^o$) and by Rodi and Zhu[39]. Fig. 12b compares for $\alpha = 0^o$ and $\alpha = 6^o$ the distribution of the friction coefficient along the bottom wall. As is well

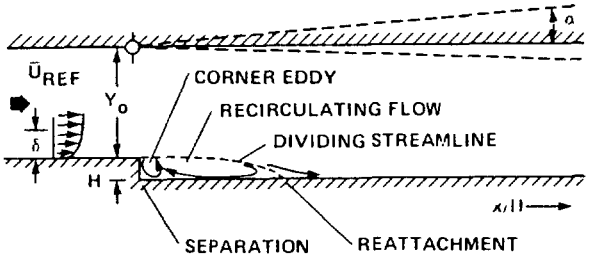

a) Flow gemoetry (from Ref. 5)

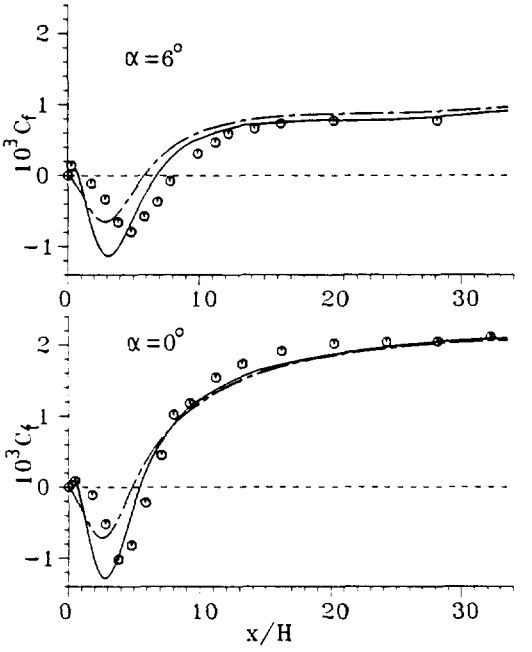

b) Friction coefficient on lower wall[39]

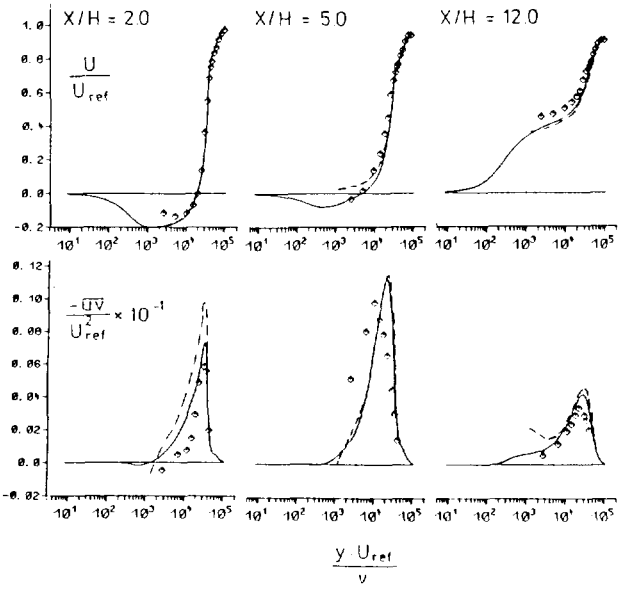

c) Velocity (U) and shear stress ($\overline{u\,v}$) profiles[22]

Fig. 12: Flow over backward facing step with aspect ratio of 1.125. Calculations[22,39]: — 2-layer model, — . —, - - - standard k-ε model, o ◊ data[5]

known, the standard k-ε model underpredicts the separation length, and this underprediction is worse for the inclined upper wall. Further, the model produces too small negative velocities and hence also c_f-values in the reverse-flow region. Application of the two-layer model brings the reattachment point much closer to the observed one but it is still about 14% short of the experimental value for the case with $\alpha = 6^o$. Also, the negative velocities are considerably stronger and are now in fact somewhat in excess of the measured ones, leading to an overprediction of negative c_f-values in the reverse-flow region. The 2-layer model calculation produced a small second corner eddy which is absent in the calculation with the standard k-ε model. Fig. 12c reveals that the two-layer model also leads to better predictions of the velocity and shear-stress profiles than the standard k-ε model. The velocity profile at x/H = 2.5 is plotted in wall coordinates in Fig. 1 and demonstrates clearly that also in the calculations without wall functions the velocity profile is far from the standard logarithmic distribution in the separated flow region. It should be mentioned here that some of the differences between two-layer and k-ε-model predictions are due to the refined near-wall resolution when the two-layer model is used.

Yap[14] has carried out heat-transfer calculations in an abrupt pipe expansion with a variety of turbulence models including a two-layer model. In the one-equation-model part of this, $\tilde{Re}_t$ was used as argument in the damping functions. When the standard k-ε model with wall functions was applied, the maximum of the Nusselt number Nu occurring near the reattachment point was overpredicted. Switching to the two-layer model produced a too low Nusselt number. This reduction in Nu is due to smaller length scales in the conduction-dominated region and the associated higher near-wall thermal resistance to heat transfer. When, on the other hand, the near-wall region was resolved by a low-Reynolds-number version of the k-ε model, the maximum Nusselt number is much higher than the observed one because the length scale near the wall is now five times higher than prescribed in the one-equation model forming part of the two-layer model. Damping of the length scale near the wall is required and Yap[14] developed a correction to the ε-equation effecting such damping. Good agreement with the experimental results was, however, only obtained in combination with an algebraic stress model instead of the k-ε eddy-viscosity model. Only then could the correct dependence of the Nusselt-number distribution on the Reynolds number be predicted.

Bühle[40] performed calculations with the two-layer and the standard k-ε model for the flow over a T-configuration studied experimentally by Jaroch and Fernholz[41]. Although these authors point out the basically three-dimensional nature of the flow in their experiment, a two-dimensional calculation was carried out for the flow in the symmetry plane. The results are shown in Fig. 13, and it can be seen again that the two-layer model predicts the reattachment length in much

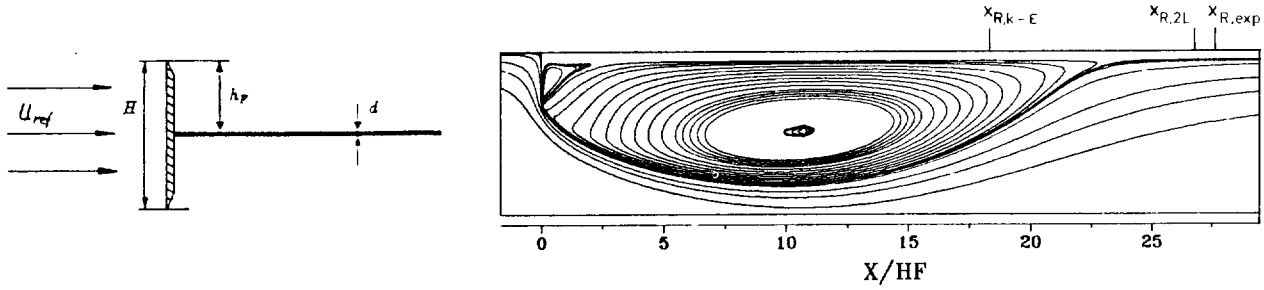

a) Flow configuration

b) Calculated streamlines in separation region

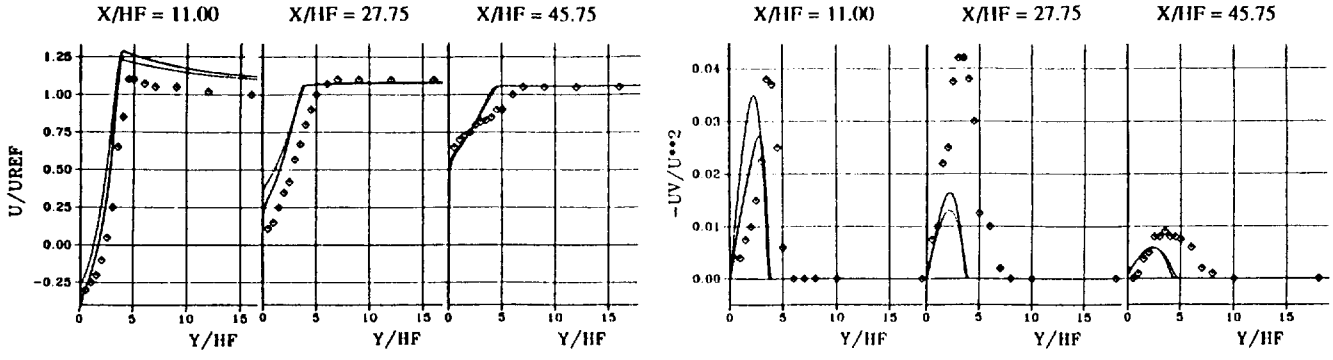

c) Velocity (U) and shear stress ($\overline{uv}$) profiles

Fig. 13: Flow over T-configuration; calculations[40]: — 2-layer model, - - - standard k-ε model, experiments[41]

better agreement with measurements than the standard k-ε model employing wall functions. On the other hand, the velocity profiles indicate that the separation zone is predicted too thin by both models. This then leads to a shift in the shear-stress distribution towards the wall. It can further be seen that the shear-stress level is underpredicted, and it is not entirely clear at present whether the higher shear stress in the experiments is associated with the basically three-dimensional nature of the flow. However, for practical purposes the overall features of the flow are reasonably well predicted by the two-layer model.

Chen and Patel[11,12] calculated the axisymmetric flow past bodies of revolution with their two-layer model. For the flow over an afterbody, whose geometry is given in Fig. 14a, the calculated friction velocity is compared with experimental data in Fig. 14b. The occurrance of a small separation region can be seen to be well reproduced by this model. Fig. 14b also includes calculations with a low-Re k-ε model, and this did not produce any separation. The results of Chen and Patel[12] for the flow over a spheroid are given in Fig. 15. The extent of the small separation region evident from the velocity vector plot in Fig. 15a is in good agreement with the flow visualisation of Chevray[43]. Fig. 15b compares calculated and measured profiles of axial velocity and turbulent kinetic energy over the rear portion of the spheroid and in the near wake. The velocity distribution is in good agreement with the data, while the turbulent kinetic energy at the trailing edge and and in the near wake is overpredicted. For better simulation in this region, the turbulence model has to be improved, e.g. by including the effects of curvature on turbulence and extending the wall damping effects into the near-wake region.

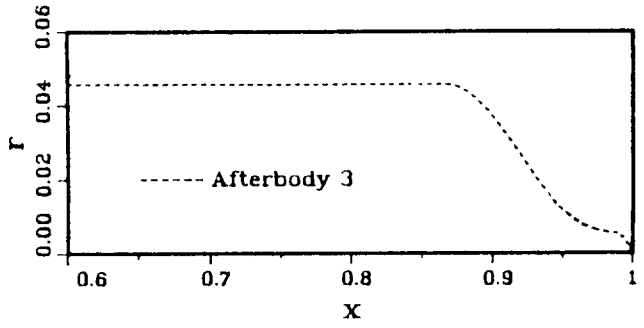

a) Geometry of body

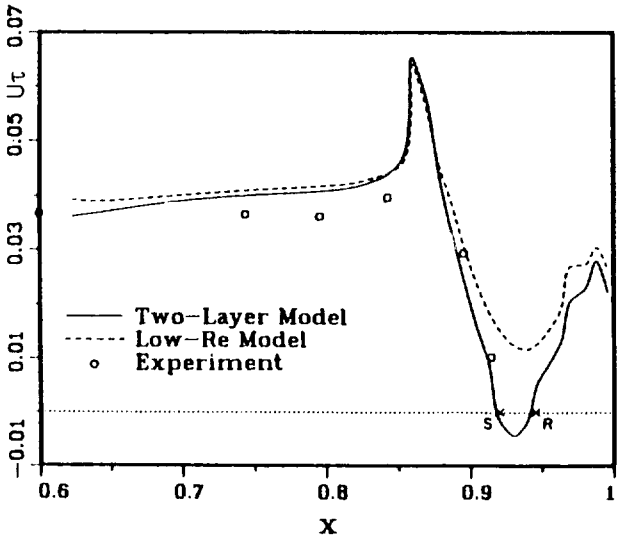

b) Friction velocity (data from Ref. 42)

Fig. 14: Flow past axisymmetric afterbody (from Ref.11)

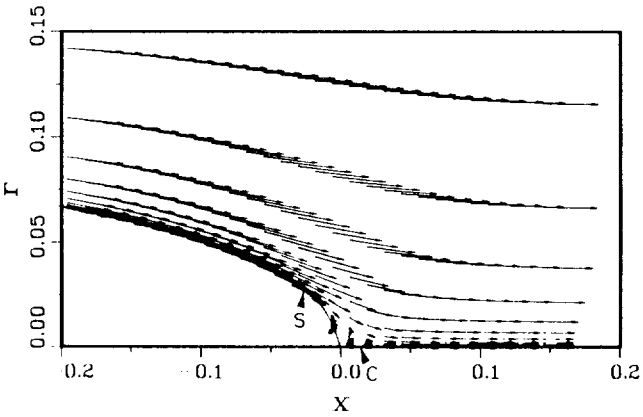

a) Calculated velocity vectors

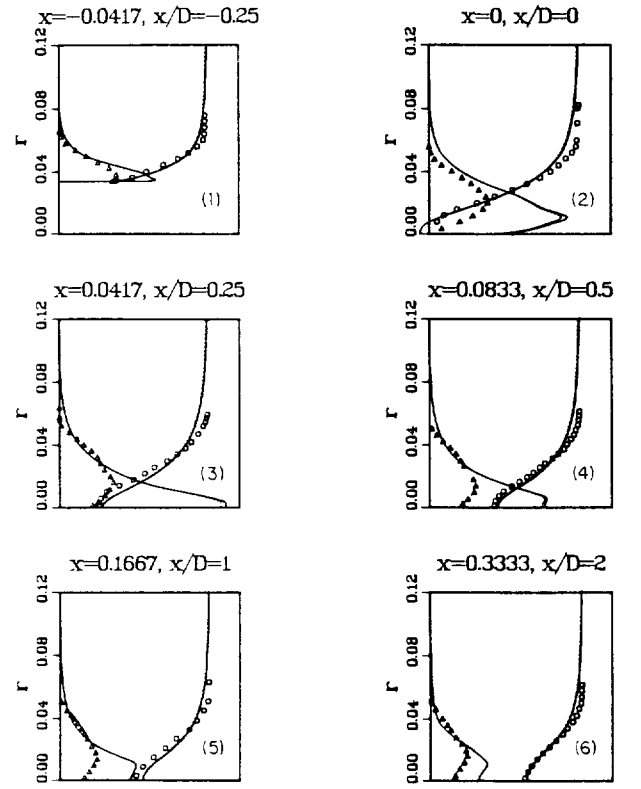

b) Velocity (o) and turbulent kinetic energy (Δ) profiles; — 2-layer model calculations, o Δ data[43]

Fig. 15: Flow past spheroid (from Ref. 12)

Cordes[22] calculated the flow over periodic dunes, in which case a sizeable recirculation zone exists. For this flow also, the two-layer model predicts correctly the size of the recirculation zone, the velocity profiles and also the wall shear stress distribution, but as in the case of the flow over a T-configuration (Fig. 13), the turbulence quantities (in particular the turbulent kinetic energy) are underpredicted. Chen and Patel[44] simulated the flow over a wavy wall with their two-layer model, including a situation where separation occurred in the trough region. The calculated distribution of the friction coefficient is in reasonable agreement with experiments.

As last example, calculations are presented for the vortex-shedding flow past a square cylinder. The periodic vortex-shedding motion is not turbulence and must be resolved in an unsteady calculation. The turbulence model has now the task to simulate the ensemble-averaged stresses appearing in the unsteady equations for the ensemble-averaged velocities. For the flow around a square cylinder at Re = 22.000, Franke[45] performed calculations with the k-ε model and the Reynolds-stress-equation model of Launder, Reece and Rodi[46], in both cases with wall functions as well as with the one-equation Norris-Reynolds[16] model for resolving the viscous sublayer. In the calculation using the k-ε model and wall functions, a steady solution resulted and now vortex shedding was obtained. The calculations with the other three model variants led to unsteady motion with periodic vortex shedding, and the calculated streamlines covering approximately one period are shown in Fig. 16a. Values of the dimensionless shedding frequencies (Strouhal number St) and time-averaged drag coefficients $\overline{c_D}$ are compared in Table 1 with experimental values. The k-ε model yields too low values for both Strouhal number and drag coefficient, while the two-layer RSE model produces too high values; the RSE model with wall functions yields results in closest agreement with the measurements, at least as far as the parameters St and $\overline{c_D}$ are concerned. Fig. 16b displays the distribution of the time-averaged velocity along the centre line, revealing that the k-ε model produces too long a separation region. This indicates that the model does not generate enough momentum exchange due to the unsteady vortex motion which is too weak in these calculations. The RSE model predicts the separation zone somewhat too short and hence this model seems to generate too much vortex shedding-shedding motion. This finding is supported by the distribution of the total (periodic plus turbulent) fluctuating energy along the centre line also shown in Fig. 16b. The total fluctuating energy predicted with the RSE model agrees fairly well with the measurements, but the turbulent contribution (not shown here) is underpredicted so that the periodic contribution must be too large. On the other hand, the k-ε model can be seen to grossly underpredict the fluctuation level behind the cylinder. In front of the cylinder, however,

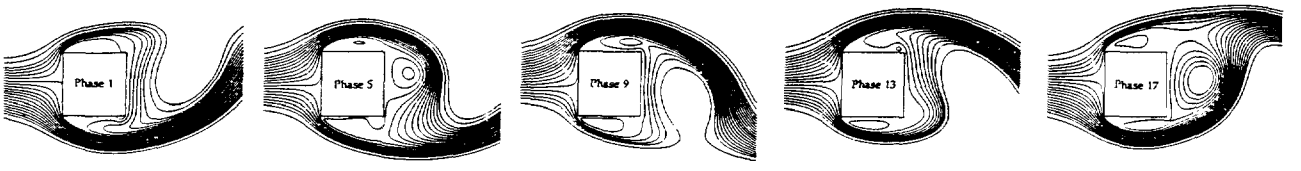

a) Streamlines calculated with 2-layer RSE model for phases t/T = 1/20, 5/20, 9/20, 13/20, 17/20

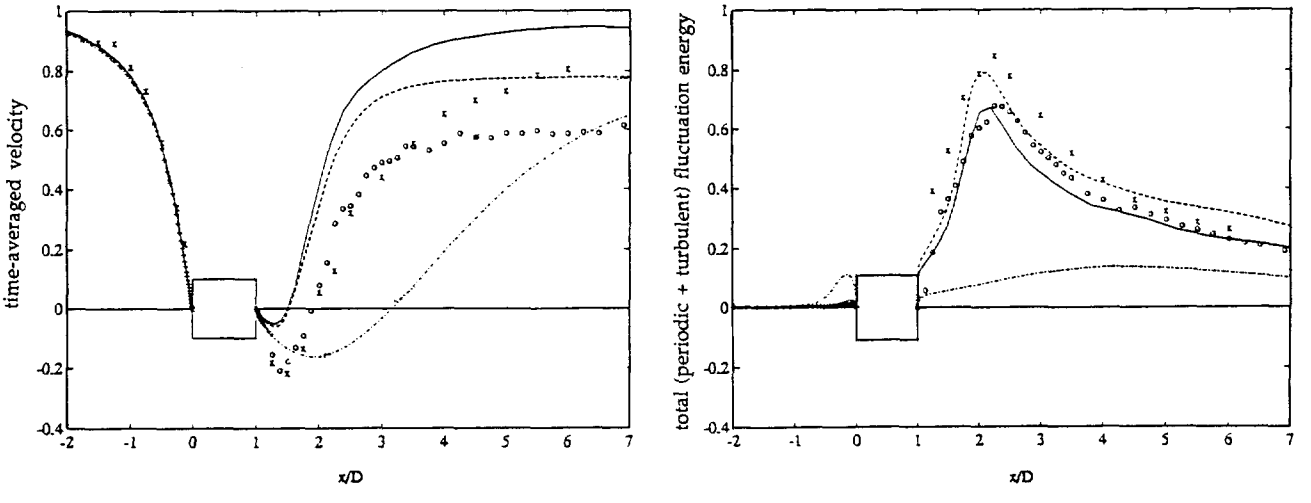

b) Distribution of time-averaged velocity and total kinetic energy along centre line.
Calculations[45]: — . — 2-layer k-ε model, — RSE model with wall functions,
- - - 2-layer RSE model; experiments: o Lyn[47] Re = 22000, x Durao et al.[48] Re = 14000

Fig. 16: Vortex shedding flow past a square cylinder; calculations[45] are for Re = 22000

Table 1 Global parameters for vortex-shedding flow past square cylinder[45]

		St	$\overline{c_D}$
Calculations	2 layer k-ε model	.124	1.79
	RSE model with wall functions	.136	2.15
	2 layer RSE model	.159	2.43
Experiments		.135-.139	2.05-2.23

the k-ε model leads to unnaturally high turbulent fluctuations. This problem with the k-ε model in stagnation flows is now well known and can be traced to the fact that the turbulent energy production in this flow is due to normal stresses (not shear stresses) and these cannot be simulated correctly with an isotropic eddy-viscosity model, leading to excessive energy production. This problem does not arise when an RSE model is used. It can be concluded here that the two-layer k-ε-based model is not suitable for vortex-shedding flow and that the use of an RSE model for the bulk of the flow leads to significantly improved predictions because it can account much better for the anisotropy, history and transport effects which are important in these flows.

3.3 Three-Dimensional Flows

A few calculations have also been carried out with two-layer for three-dimensional flows, but these can only be briefly listed here. Launder and co-workers[49,50] have calculated the flow in ducts of various geometries. Piquet and Visonneau[51] have applied a two-layer model in their calculation of the flow around a ship and Deng et al.[52] used the same model for calculating 3D flow on a flat-plate junction and on a prolate spheroid at incidence. In general, encouraging results were obtained in these 3D calculations.

4. Concluding Remarks

The two-layer approach in turbulence modelling has recently become popular at various research institutions. In this approach, the bulk of the flow is simulated with models employing a length-scale-determining equation, ranging from the k-ε eddy-viscosity model to Reynolds-stress-equation (RSE) models, while the viscosity-affected near-wall region is resolved with a simpler one-equation model employing a prescribed length-scale distribution. The paper has concentrated on two-layer models in which the bulk of the flow is calculated with the k-ε model. Independent developments at different research groups led to the use of somewhat different damping functions in the length-scale prescription of the one-equation models and also to different practices for matching the two models. A systematic study on the influence of these differences is not available.

The application examples presented for a variety of two-dimensional boundary-layer and separated flows have shown that the results obtained with the two-layer model are very encouraging. For boundary layers, the predictions are generally as good as those obtained with low-Re k-ε models, and for situations with adverse-pressure gradient they are better, while fewer grid points are required. It was also shown that transitional boundary layers can be predicted reasonably well with the aid of empirical transition relations entering one of the damping functions in the one-equation model. For steady separated flows, the two-layer-model results are clearly improved over those obtained with the k-ε model employing wall functions; most notably larger, more realistic separation regions are predicted. For the example with unsteady vortex shedding, the k-ε based two-layer model severely underpredicts the periodic shedding motion and an RSE model is necessary for a realistic simulation of this motion, and here also the two-layer approach appears promising. With the computing power now available, three-dimensional calculations with two-layer models seem also possible with say 10 to 15 grid points in the near-wall region where the one-equation model is effective. Hence, these models are promising tools for practical calculations in situations where wall functions are either not applicable or inaccurate and where low-Reynolds-number versions of the outer-flow model are not well behaved or too costly.

5. Acknowledgements

The work reported here was supported partly by the Deutsche Forschungsgemeinschaft. The author is grateful to J. Cordes, R. Franke, D. Lyn and J. Zhu for providing unpublished results and to R. Zschernitz for the efficient typing of the manuscript.

6. References

1. Launder, B.E. and Spalding, D.B., "The numerical computation of turbulent flow", Comp. Meth. in Appl. Mech. and Eng., **3**, 1974, pp. 269-289.
2. Iacovides, H. and Launder, B.E., "The numerical simulation of flow and heat transfer in tubes in orthogonal-mode rotation", Proc. 6th Symp. on Turbulent Shear Flows, Toulouse, France, 1987.
3. Adams, E.W. and Johnston, J.P., "Flow structure in the near-wall zone of a turbulent separated flow", AIAA J., **26**, pp. 932-939.
4. Ruderich, R. and Fernholz, H.H., "An experimental investigaton of a turbulent shear flow with separation, reverse flow, and reattachment", J. Fluid Mech., **163**, 1986, pp. 283-322.
5. Driver, D.M. and Seegmiller, H.J., "Features of reattaching turbulent shear layer in divergent channel flow", AIAA J., **23**, 1985, pp. 163-171.
6. Launder, B.E., "Low-Reynolds number turbulence near walls", UMIST, Manchester, Dept. of Mech. Eng. Rept. TFD/86/4, 1986.
7. Patel, V.C., Rodi, W. and Scheuerer, G., "Turbulence models for near-wall and low-Reynolds-number flows: A review", AIAA J., **23**, 1985, pp. 1308-1319.
8. Shih, T.H. and Mansour, N.N., "Modelling of near-wall turbulence", in *Engineering Turbulence Modelling and Experiments*, eds. W. Rodi and E.N. Ganic', Elsevier, 1990, pp. 13-22.
9. Rodi, W. and Scheuerer, G., "Calculation of heat transfer to convection-cooled gas turbine blades", ASME J. Engineering for Gas Turbines and Power, **107**, 1985, pp. 620-627.
10. Rodi, W. and Scheuerer, G., "Scrutinizing the k-ε model under adverse pressure gradient conditions", J. Fluids Eng., **108**, 1986, pp. 174-179.
11. Chen, H.C. and Patel, V.C., "Near-wall turbulence models for complex flows including separation", AIAA J., **26**, 1988, pp. 641-648.

12. Chen, H.C. and Patel, V.C., "Evolution of axisymmetric wakes from attached and separated flows", in *Turbulent Shear Flows 6*, Springer Verlag, 1989, pp. 215-231.

13. Wolfshtein, M., "The velocity and temperature distribution in one-dimensional flow with turbulence augmentation and pressure gradient", Int. J. Heat Mass Transfer, **12**, 1969, pp. 301-318.

14. Yap, C.L., "Turbulent heat and momentum transfer in recirculating and impinging flows", Ph.D. Thesis, UMIST, Manchester, 1987.

15. Iacovides, H. and Launder, B.E., "Parametric and numerical study of fully-developed flow and heat transfer in rotating rectangular ducts", ASME Paper 90/GT/24, 1990.

16. Norris, L.H. and Reynolds, W.C., "Turbulent channel flow with a moving wavy boundary", Rept. No. FM-10, Stanford University, Dept. Mech. Eng., 1975.

17. Rodi, W., "Examples of turbulence-model applications", in *Turbulence Models and Their Applications*, édition Eyrolles, Paris, 1984, pp. 295-401.

18. Fujisawa, N., Rodi, W. and Schönung, B., "Calculation of transitional boundary layers with a two-layer model of turbulence", Proc. 3rd Int. Symp. on Transport Phenomena and Dynamics of Rotating Machinery, Honolulu, April 1990.

19. Durbin, P.A., "Near-wall turbulence closure modelling without damping functions", CTR Manuscript 112, Center for Turbulence Research, Stanford University, 1990.

20. Rodi, W. and Mansour, N.N., "One-equation near-wall turbulence modelling with the aid of direct simulation data", Proc. 1990 Summer Program of Center for Turbulence Research, Stanford University, 1990.

21. Mansour, N.N. , Kim, J. and Moin, P., "Reynolds-stress and dissipation-rate budgets in a turbulent channel flow", J. Fluid Mech., **194**, 1988, pp. 15-44.

22. Cordes, J., "Entwicklung und Anwendung eines Zweischichten-Turbulenzmodells für abgelöste zweidimensionale Strömungen", Ph.D. Thesis, University of Karlsruhe, 1991.

23. Coles, D. and Hirst, E.A., *Proceedings Computation of Turbulent Boundary Layers, 1968 AFOSR-IFP Stanford Conference*, Vol. 2, Thermosc. Div., Dept. Mech. Eng., Stanford University, 1969.

24. Klebanoff, P.S., "Characteristics of turbulence in a boundary layer with zero pressure gradient", NACA-TN 3178, 1954.

25. Patel, V.C., Calculations communicated to organisers of Collaborative Testing of Turbulence Models, 1990.

26. Spalart, P.R, "Direct simulation of a turbulent boundary layer up to $R\theta$ = 1410", J. Fluid Mech., **187**, 1988, pp. 61-98.

27. Samuel, A.E. and Joubert, P.M., "A boundary layer developing in an increasingly adverse pressure gradient", J. Fluid Mech., **66**, 1974, pp. 481-505.

28. Bradshaw, P., "The turbulence structure of equilibrium boundary layers", J. Fluid Mech., **29**, 1967, pp. 625-645.

29. Patel, V.C. and Richmond, M.C., "Pressure gradient and surface curvature effects in turbulent boundary layers", Paper AIAA-87-1301, 1987.

30. Badri Narayanan, M.A. and Ramjee, V., "On the criteria for reverse transition in a two-dimensional boundary layer flow", J. Fluid Mech., **35**, 1969, pp. 225-241.

31. Rodi, W., "Examples of turbulence models for incompressible flows", AIAA J., **20**, 1982, pp. 872-879.

32. Crawford, M.E. and Kays, M.W., "STAN 5 - a program for numerical computation of two-dimensional internal and external boundary-layer flows", NASA CR-2742, 1976.

33. Abu Ghannam, B.J. and Shaw, R. "Natural transition of boundary layers - the effects of turbulence, pressure gradient and flow history", J. Mech. Eng. Sci., **22**, 1980, pp. 213-228.

34. Rodi, W., Fujisawa, N. and Schönung, B., "Calculation of transitional boundary layers under the influence of free-stream turbulence", in Proc. ERCOFTAC Workshop on Numerical Simulation of Unsteady Flows, Transition to Turbulence and Combustion, Cambridge University Press, 1991.

35. Savill, M., "Introduction to test case T3", in Proc. ERCOFTAC Workshop on Numerical Simulation of Unsteady Flows, Transition to Turbulence and Combustion, Cambridge University Press, 1991.

36. Blair, M.F. and Werle, M.J., "The influence of free-stream turbulence on the zero pressure gradient fully turbulent boundary layer", UTRC Rept. R80-914388-12, 1980.

37. Blair, M.F. and Werle, M.J., "Combined influence of free-turbulence and favourable pressure gradients on boundary-layer transition and heat transfer", UTRC Rept. R81-914388-17, 1981.

38. Rodi, W., Liu, X. and Schönung, B., "Transitional boundary layers with wake-induced unsteadiness", Proc. 4th Symp. on Numerical and Physical Aspects of Aerodynamic Flows, Long Beach, California, January 1989.

39. Rodi, W. and Zhu, J., Calculations communicated to organisers of Collaborative Testing of Turbulence Models, 1990.

40. Bührle, P., "Numerische Berechnung der abgelösten Strömung über eine senkrechte ebene Platte mit einer zur Anströmung parallelen Trennplatte in der Symmetrieebene", Studienarbeit am Institut für Hydromechanik, Universität Karlsruhe, 1989.

41. Jaroch, M.P. and Fernholz, H.H., "The three-dimensional character of a nominally two-dimensional separated turbulent shear flow", J. Fluid Mech., **205**, 1989, pp. 523-552.

42. Huang, T.T., Groves, M.C. and Belt, G., "Boundary-layer flow on an axisymmetric body with an inflected stern", David W. Taylor Naval Ship Research and Development Center, Rept. 80-064, 1980.

43. Chevreay, R., "The turbulent wake of a round body, ASME J. Basic Eng., **90**, 1968, pp. 275-284.

44. Chen, J.T. and Patel, V.C., "A numerical study of turbulent flow in a channel with wavy wall", Proc. 10th Australian Fluid Mechanics Conference, Melbourne, Dec. 1989.

45. Franke, R., "Numerische Berechnung der instationären Wirbelablösung hinter zylindrischen Körpern", Ph.D. Thesis, University of Karlsruhe, 1991.

46. Launder, B.E., Reece, G.J. and Rodi, W., "Progress in the development of a Reynolds-stress turbulence closure", J. Fluid Mech., **68**, 1975, pp. 537-566.

47. Lyn, D., private communication, 1989.

48. Durao, D.F.G., Heitor, M.V. and Pereira, J.C.F., "Measurements of turbulent and periodic flows around a square cross-sectioned cylinder", Experiments in Fluids, **6**, 1988, pp. 298-304.

49. Launder, B.E. and Loizou, P.A., "Laminarisation in three-dimensional accelerating flow through curved rectangular ducts", Proc. 7th Symp. on Turbulent Shear Flows, Stanford University, August 1989, pp. 28.2.1-28.2.6.

50. Leschziner, M.A., Launder, B.E. and Iacovides, H., "Application and evaluation of 3D finite volume RANS schemes in turbulent aerodynamic flows - phase 2", Rept. FLAIR/90/1, UMIST, Manchester, Feb. 1990.

51. Piquet, J. and Visonneau, M., "Computation of the flow past ship-like hulls", to appear in Computers in Fluids, 1991.

52. Deng, G.B., Piquet, J. and Visonneau, M., "Navier-Stokes computations of vortical flows", AIAA Paper 90-1628, 1990.